

Available online at www.sciencedirect.com

ScienceDirect

journal homepage: <http://www.elsevier.com/locate/acme>

Original Research Article

Navier–Stokes problems with random coefficients by the Weighted Least Squares Technique Stochastic Finite Volume Method

M. Kamiński*, R.L. Ossowski

Department of Structural Mechanics, Technical University of Łódź, Al. Politechniki 6, 90-924 Łódź, Poland

ARTICLE INFO

Article history:

Received 10 May 2013

Accepted 14 December 2013

Available online 14 January 2014

Keywords:

Stochastic Finite Volume Method
 Generalized stochastic perturbation technique
 Weighted Least Squares Method
 Navier–Stokes equations
 Symbolic computing

ABSTRACT

The main aim of this article is numerical solution to the Navier–Stokes equations for incompressible, non-turbulent and subsonic fluid flows with Gaussian physical random parameters. It is done with the use of the specially adopted Finite Volume Method extended towards probabilistic analysis by the generalized stochastic perturbation technique. The key feature of this approach is the weighted version of the Least Squares Method implemented symbolically in the system MAPLE to recover nodal polynomial response functions of the velocities, pressures and temperatures versus chosen input random variable(s). Such an implementation of the Stochastic Finite Volume Method is applied to model 3D flow problem in the statistically homogeneous fluid with uncertainty in its viscosity and, separately, coefficient of the heat conduction. Probabilistic central moments of up to the fourth order and the additional characteristics are determined and visualized for the cavity lid driven flow owing to the specially adopted graphical environment FEPlot. Further numerical extension of this technique is seen in an application of the Taylor–Newton–Gauss approximation technique, where polynomial approximation may be replaced with the exponential or hyperbolic ones.

© 2013 Politechnika Wroclawska. Published by Elsevier Urban & Partner Sp. z o.o. All rights reserved.

1. Introduction

Computational solution of the fully coupled Navier–Stokes equations is still really challenging problem, especially when defined in terms of random coefficients. We prefer the generalized stochastic perturbation technique as it allows for a determination of third and fourth central moments as well as such coefficients like skewness and/or kurtosis. Instead of a time consuming implementation of the Direct Differentiation Method (DDM), the Response Function Method (RFM) is

preferred, so that instead of up to the n th order coupled Navier–Stokes equations we solve for some polynomial approximations of the state functions relating the PVT solution with the input random variable(s). This approximation is proposed here in a local sense – the response functions for velocities, pressures and temperatures may be different in each discrete point of the computational domain. This idea is connected here with the classical deterministic formulation of the Finite Volume Method (FVM) [2–4]. A very useful property of the FVM is that the conservation principles, which are the basis for the mathematical modeling of continuum mechanical problems are also

* Corresponding author.

E-mail addresses: Marcin.Kaminski@p.lodz.pl, mm_kaminski@wp.pl (M. Kamiński).URL: <http://www.kmk.p.lodz.pl/pracownicy/kaminski/index.htm>

Notation

Roman symbols

c	specific heat
d_j	direction vector
f_i	body forces per unit volume
g	gravitational acceleration
k	thermal conductivity
n_s	number of the finite volume outer faces
p	fluid pressure
$p_b(x)$	probability density function
q_i	the heat flux
t	time parameter
v_i	velocity vector
A_j	an area the face j of the given finite volume
$E[b]$	expected value of random variable b
$D_{\beta m}^p$	matrix of unknown polynomial coefficients for pressure response
$D_{\beta m}^T$	matrix of unknown polynomial coefficients for temperature response
$D_{\beta m}^U$	matrix of unknown polynomial coefficients for velocity response
$K_1^{P(\alpha)}, \bar{K}_{ij}^{P(\alpha)}$	system matrices for the pressures corresponding to the l th finite volume center and the center of its j th outer face, α th RFM test
$K_1^{T(\alpha)}, \bar{K}_{ij}^{T(\alpha)}$	system matrices for the temperatures corresponding to the l th finite volume center and the center of its j th outer face, α th RFM test
$K_1^{U(\alpha)}, \bar{K}_{ij}^{U(\alpha)}$	system matrices for the velocities corresponding to the l th finite volume center and the center of its j th outer face, α th RFM test
M	total number of deterministic experiments necessary for the response function recovery
N	total number of degrees of freedom in the system
P	vector of discrete pressures
$P_1^{(\alpha)}(t)$	pressure in the center of finite volume l at time t , α th RFM test
$\bar{P}_{ij}^{(\alpha)}(t)$	pressure face flux (finite volume l , its j outer plane, at time t , α th RFM test)
$Q_i^{P(\alpha)}, Q_i^{U(\alpha)}, Q_i^{T(\alpha)}$	the R.H.S. vectors for the pressures, velocities and temperatures at the l th finite volume and α th RFM test
S_j	normal vector
T	discrete temperatures vector
$T_1^{(\alpha)}(t)$	temperature of the center of finite volume l at time t , α th RFM test
$\bar{T}_{ij}^{(\alpha)}(t)$	temperature face flux (finite volume l , its j outer plane, at time t , α th RFM test)
U	the vector of discrete velocities
$U_1^{(\alpha)}(t)$	velocity of the center of finite volume l at time t , α th RFM test
$\bar{U}_{ij}^{(\alpha)}(t)$	velocity face flux (finite volume l , its j outer plane, at time t , α th RFM test)
V_l	total volume of the l th sub-volume
$\text{Var}(b)$	variance of random variable b

Greek symbols

α, β	the local index symbol
$\alpha(b)$	the coefficient of variation of random variable b
$\beta(b)$	skewness coefficient of random variable b
$\kappa(b)$	kurtosis of random variable b
δ_{ij}	Kronecker delta
ε_{ij}	strain tensor
ε	perturbation parameter
ρ	fluid density
μ	fluid viscosity
$\mu_p(b)$	p th central moment of the variable b
σ_{ij}	stress tensor
χ	interpolation coefficient
θ	temperature
$\phi_l^{(\alpha)}$	viscous dissipation for the l th finite volume and α th RFM numerical test
φ_β	shape functions
$(\dots)_i$	partial derivative symbol
Δt	time increment

fulfilled for the discrete equations [8]. A starting point for the FVM is a decomposition of the problem domain into both regular and irregular sub-volumes, where each such a sub-volume is represented by its midpoint only. This is the main difference to the Finite Element Method (FEM) [5,8], where the equilibrium equations are formed and solved in the nodal points of the mesh only, which are located in the corners (and midpoints for higher order approximations) of each finite element.

Computational analysis is provided in a hybrid way here – the FVM freeware code OpenFVM is engaged to solve all N-S problems necessary to build up the response functions. The internal symbolic Least Squares Method of the system MAPLE accompanied with the perturbation-based formulas implemented in this program leads to the final statistical moments of the fluid state. We recommend the weighted version of the LSM, where each discretization point to define variability of the input random quantity has some associated weight showing its contribution to the final expected value. Numerical visualization is carried out in the freeware FEPlot used before for the FEM and FDM output files and procedures. Computational illustration deals with incompressible fluid flow in a cubic domain and this flow occurs with two Gaussian input random variables – heat conductivity coefficient and, separately, fluid viscosity. We compute twice up to fourth order probabilistic characteristics of the PVT solution to validate an importance of both physical parameters. Although these input parameters are state-independent, further extension of the proposed SFVM toward numerical modeling of nonlinear, i.e. temperature-dependent systems will be also possible.

2. Governing equations

2.1. Navier–Stokes equations

The system of basic equilibrium equations to be extended toward stochastic analysis and to be solved numerically can be written with boundary conditions as follows [2,6,7]:

$$\rho \left(\frac{\partial v_i}{\partial t} + v_{i,j} v_j \right) = \sigma_{ij,j} + \tilde{f}_i, \tag{1}$$

$$v_{i,i} = 0, \tag{2}$$

$$\sigma_{ij} = -p \delta_{ij} + 2\mu \varepsilon_{ij}, \tag{3}$$

$$\rho c \left(\frac{\partial \theta}{\partial t} + \theta_{,i} v_i \right) = (k \theta_{,i})_{,i} + \tilde{q}_i, \tag{4}$$

where the following notation is adopted:

$$\varepsilon_{ij} = \frac{1}{2} (v_{i,j} + v_{j,i}) = \frac{1}{2} \left(\frac{\partial v_i}{\partial x_j} + \frac{\partial v_j}{\partial x_i} \right), \quad i = 1, 2, 3. \tag{5}$$

State variables in Eqs. ((1)–(5)) show successively the velocities (v_i), pressure (p) of the analyzed fluid, the stress (σ_{ij}) and strain (ε_{ij}) tensors as well as the temperature distribution (θ). The uncertainty analysis provided in this work concerns physical parameters of the fluid, i.e. viscosity (μ) and heat conductivity (k), separately, but may also represent heat capacity (c) or mass density (ρ) of this fluid.

Let us complete this system with the following boundary conditions:

- for the velocity

$$v_i = \hat{v}_i; \quad \mathbf{x} \in \partial\Omega_v, \tag{6}$$

- for the stress tensor

$$\sigma_{ij} n_j = \hat{f}_i; \quad \mathbf{x} \in \partial\Omega_\sigma, \tag{7}$$

- for the temperature

$$\theta = \hat{\theta}; \quad \mathbf{x} \in \partial\Omega_\theta \tag{8}$$

- and for the heat flux

$$k \frac{\partial \theta}{\partial \mathbf{x}} = \hat{q}; \quad \mathbf{x} \in \partial\Omega_q. \tag{9}$$

For the numerical solution of differential equations above we apply variational formulation, where the equations are numerically integrated over the given volume Ω . This operation allows to obtain the starting equations of thermodynamic equilibrium in the following notation:

$$\int_{\Omega} \delta v_i \rho (\hat{v}_i + v_{i,j} v_j) d\Omega + \int_{\Omega} \delta v_{i,j} (2\mu \varepsilon_{ij} - p \delta_{ij}) d\Omega = \int_{\Omega} \delta v_i \tilde{f}_i d\Omega + \int_{\partial\Omega} \delta v_i \hat{f}_i d(\partial\Omega_\sigma), \tag{10}$$

$$\int_{\Omega} \delta p v_{i,i} d\Omega = 0, \tag{11}$$

$$\int_{\Omega} \delta \theta \rho c (\hat{\theta} + \theta_{,i} v_i) d\Omega + \int_{\Omega} k \delta \theta_{,i} \theta_{,i} d\Omega = \int_{\Omega} \delta \theta \hat{q} d\Omega + \int_{\partial\Omega_q} \delta \theta \hat{q} d(\partial\Omega). \tag{12}$$

Eqs. ((10)–(12)) are all transformed using the generalized stochastic perturbation method and discretized by the Finite Volume Method scheme for a numerical solution of the unsteady coupled fluid flow problem with random physical parameters. Some analytical techniques leading to the solution of at least last equation, Eq. (12) are available in [1].

2.2. The generalized stochastic perturbation method

Let us consider the random variable b and its probability density function (PDF) by $p_b(x)$, so that its expectation can be defined as

$$E(b) = \int_{-\infty}^{+\infty} b p_b(x) dx \tag{13}$$

assuming no additional truncation on this variable. Further, one can define the central probabilistic moment of the m th order for this variable as

$$\mu_m(b) = \int_{-\infty}^{+\infty} (b - E[b])^m p_b(x) dx. \tag{14}$$

Let us note that b represents further some physical parameters of the system as well as their state functions like temperatures, pressures or fluid velocities and usually has arbitrarily chosen Gaussian distribution truncated according to its physical meaning. As it is known [5–7], the basic idea of the stochastic perturbation approach follows the classical perturbation expansion idea and is based on approximation of all input variables, and the state functions of the problem via the truncated Taylor series about their spatial expectations. Let us consider the following representation of the random function $\mathbf{v}(b)$ with respect to its parameter b around its mean value:

$$\mathbf{v}(b) = \mathbf{v}^0(b^0) + \varepsilon \frac{\partial \mathbf{v}(b)}{\partial b} \Big|_{b=b^0} \Delta b + \dots + \frac{\varepsilon^n}{n!} \frac{\partial^n \mathbf{v}(b)}{\partial b^n} \Big|_{b=b^0} \Delta b^n, \tag{15}$$

where ε is a given perturbation parameter (adopted here as equal to 1), while the n th order variation of random variable is given as follows:

$$\varepsilon^n \Delta b^n = (\delta b)^n = \varepsilon^n (b - b^0)^n. \tag{16}$$

Let us note that this expansion procedure may be used with some small modifications by only for the few random variables (the vector with the few coordinates) – for both correlated and uncorrelated quantities. Then, the same expansions are provided and the cross-correlations terms will additionally appear in the equations describing basic moments and characteristics of the state functions (cf. [5]). The expected values are sufficiently accurate with the use of the 10th order expansion and for $\varepsilon = 1$ (assumed for all further derivations) as

$$E[\mathbf{v}(b)] = \mathbf{v}^0(b^0) + \frac{1}{2} \frac{\partial^2 \mathbf{v}(b)}{\partial b^2} \Big|_{b=b^0} \mu_2(b^0) + \frac{1}{4!} \frac{\partial^4 \mathbf{v}(b)}{\partial b^4} \Big|_{b=b^0} \mu_4(b^0) + \frac{1}{6!} \frac{\partial^6 \mathbf{v}(b)}{\partial b^6} \Big|_{b=b^0} \mu_6(b^0) + \frac{1}{8!} \frac{\partial^8 \mathbf{v}(b)}{\partial b^8} \Big|_{b=b^0} \mu_8(b^0) + \frac{1}{10!} \frac{\partial^{10} \mathbf{v}(b)}{\partial b^{10}} \Big|_{b=b^0} \mu_{10}(b^0) \tag{17}$$

for any natural m with μ_{2m} being the ordinary probabilistic moment of $2m$ th order. This expansion is justified for the symmetric probability distribution functions, like the Gaussian one, where all odd orders simply vanish. Analogous observation significantly simplifies algebraic equations for higher central moments also, although full perturbation-based expansions (with both even and odd order terms are available in the literature, see [5]). Further, according to some previous computational convergence studies, we may limit this

expansion to the 10th order for all the moments of an interest here. Quite similar considerations lead to the expressions for higher moments, like the variance, for instance

$$\begin{aligned}
 \text{Var}(\mathbf{v}(b)) &= \mu_2(\mathbf{v}(b)) \\
 &= \int_{-\infty}^{+\infty} (\mathbf{v}(b) - E[\mathbf{v}(b)])^2 p_b(x) dx \\
 &= \mu_2(b^0) \left(\frac{\partial \mathbf{v}(b)}{\partial b} \Big|_{b=b^0} \right)^2 \\
 &+ \mu_4(b^0) \left\{ \frac{1}{4} \left(\frac{\partial^2 \mathbf{v}(b)}{\partial b^2} \Big|_{b=b^0} \right)^2 + \frac{1}{3} \frac{\partial^3 \mathbf{v}(b)}{\partial b^3} \Big|_{b=b^0} \frac{\partial \mathbf{v}(b)}{\partial b} \Big|_{b=b^0} \right\} \\
 &+ \mu_6(b^0) \left\{ \frac{1}{36} \left(\frac{\partial^3 \mathbf{v}(b)}{\partial b^3} \Big|_{b=b^0} \right)^2 + \frac{1}{24} \frac{\partial^4 \mathbf{v}(b)}{\partial b^4} \Big|_{b=b^0} \frac{\partial^2 \mathbf{v}(b)}{\partial b^2} \Big|_{b=b^0} \right. \\
 &+ \left. \frac{1}{60} \frac{\partial^5 \mathbf{v}(b)}{\partial b^5} \Big|_{b=b^0} \frac{\partial \mathbf{v}(b)}{\partial b} \Big|_{b=b^0} \right\} \\
 &+ \mu_8(b^0) \left\{ \frac{1}{576} \left(\frac{\partial^4 \mathbf{v}(b)}{\partial b^4} \Big|_{b=b^0} \right)^2 \right. \\
 &+ \left. \frac{1}{360} \frac{\partial^5 \mathbf{v}(b)}{\partial b^5} \Big|_{b=b^0} \frac{\partial^3 \mathbf{v}(b)}{\partial b^3} \Big|_{b=b^0} \right\} \\
 &+ \mu_8(b^0) \left\{ \frac{1}{2520} \frac{\partial^7 \mathbf{v}(b)}{\partial b^7} \Big|_{b=b^0} \frac{\partial \mathbf{v}(b)}{\partial b} \Big|_{b=b^0} \right. \\
 &+ \left. \frac{1}{720} \frac{\partial^6 \mathbf{v}(b)}{\partial b^6} \Big|_{b=b^0} \frac{\partial^2 \mathbf{v}(b)}{\partial b^2} \Big|_{b=b^0} \right\} \\
 &+ \mu_{10}(b^0) \left\{ \frac{1}{14400} \left(\frac{\partial^5 \mathbf{v}(b)}{\partial b^5} \Big|_{b=b^0} \right)^2 \right. \\
 &+ \left. \frac{1}{40320} \frac{\partial^8 \mathbf{v}(b)}{\partial b^8} \Big|_{b=b^0} \frac{\partial^2 \mathbf{v}(b)}{\partial b^2} \Big|_{b=b^0} \right\} \\
 &+ \mu_{10}(b^0) \left\{ \frac{1}{8640} \frac{\partial^6 \mathbf{v}(b)}{\partial b^6} \Big|_{b=b^0} \frac{\partial^4 \mathbf{v}(b)}{\partial b^4} \Big|_{b=b^0} \right\} \\
 &+ \mu_{10}(b^0) \left\{ \frac{1}{15120} \frac{\partial^7 \mathbf{v}(b)}{\partial b^7} \Big|_{b=b^0} \frac{\partial^3 \mathbf{v}(b)}{\partial b^3} \Big|_{b=b^0} \right. \\
 &+ \left. \frac{1}{181440} \frac{\partial^9 \mathbf{v}(b)}{\partial b^9} \Big|_{b=b^0} \frac{\partial \mathbf{v}(b)}{\partial b} \Big|_{b=b^0} \right\} \tag{18}
 \end{aligned}$$

Third and fourth probabilistic moment may be recovered from this scheme quite similarly and are included together with a discussion of the probabilistic convergence of the entire method in [5]. The central moments of the variable b may be obviously simply recovered here as

$$\mu_p(b) = \begin{cases} 0; & p = 2k + 1 \\ \{\sigma(b)\}^p (p-1)!! = \{\sigma(b)\}^p (p-1) \cdot (p-3) \dots 5 \cdot 3; & p = 2k \end{cases} \tag{19}$$

for any natural $k \geq 1$, which is the consequence of the Gaussian distribution symmetry. As one may suppose, the higher order moments we need to compute the higher order perturbations need to be included into all formulas, so that the complexity of the computational model grows non-proportionally together with the precision and the size of the output information needed.

3. The Stochastic Finite Volume Method

Now the goal would be to compute up to n th order velocities, pressures and temperatures and calculate their first four

statistical moments and coefficients. Because of an unknown computational error resulting from up to n th order equilibrium equations and the direct access to the source code we propose the Response Function Method where some polynomial approximation of the state function (like temperatures below) in a given sub-volume center with respect to the input random variable b is proposed in the following form [5]:

$$T_\beta = D_{\beta m}^T b^m, m = 0, \dots, n-1; \quad \beta = 1, \dots, N. \tag{20}$$

where $D_{\beta m}^T$ is a rectangular matrix of the unknown polynomial coefficients, so that there holds

$$\begin{aligned}
 \theta(x_i) &= \varphi_\beta(x_i) T_\beta = \varphi_\beta(x_i) D_{\beta m}^T b^m; \quad i = 1, 2, \dots, N; \quad m \\
 &= 0, \dots, n-1, \end{aligned} \tag{21}$$

where φ_β are traditional deterministic shape functions and T_β is a vector of the unknown discrete temperatures in the system (we discretize similarly the pressures and velocities using the vectors \mathbf{P} and \mathbf{U} respectively).

An idea of such an approximation of the random state functions is somewhat similar to the well-known polynomial chaos approach, but instead of the series of polynomials of lower order defined for the few random variables we apply a single variable and higher order representation for all the state functions, separately. It is done in the local formulation, where such a polynomial representation varies on the given degree of freedom and a specific node in computational grid. Coupled Navier–Stokes problem having triple solutions (P, U, T) needs three different matrices $D_{\beta m}^P, D_{\beta m}^U$ and $D_{\beta m}^T$ containing unknown polynomial coefficients to be determined.

Therefore, the temperature gradients are similarly determined as

$$\theta_{,j} = \varphi_{\beta,j} T_\beta = \varphi_{\beta,j} D_{\beta m}^T b^m, \quad i = 1, 2, m = 0, \dots, n-1. \tag{22}$$

Analogous representation is proposed for the pressures

$$P_\beta = D_{\beta m}^P b^m, m = 0, \dots, n-1; \quad \beta = 1, \dots, N. \tag{23}$$

and velocities. It needs to be recalled that the discrete velocity vector has three times more components than these corresponding to the pressures and temperatures. Contrary to the Finite Element Method and its stochastic perturbation-based implementation we rewrite right now this polynomial approximation for each finite volume separately (having each n_s outer surfaces). Generally, the approximating polynomial orders for the PVT solution components do not need to be exactly the same – this choice is affected mainly by the uncertainty source and physical interpretation in the given problem. Final recovery of the local approximations for the state functions results from several trial solutions using the classical FVM around the mean value of the random input parameters. So that typical discretization is enriched with the new upper index $\alpha = 1, \dots, M$ (inserted further in the brackets), where M denotes the total number of computational experiments necessary to recover the response function (usually around 10). We need to emphasize that the discretization method applied here assumes the parameter n_s as constant

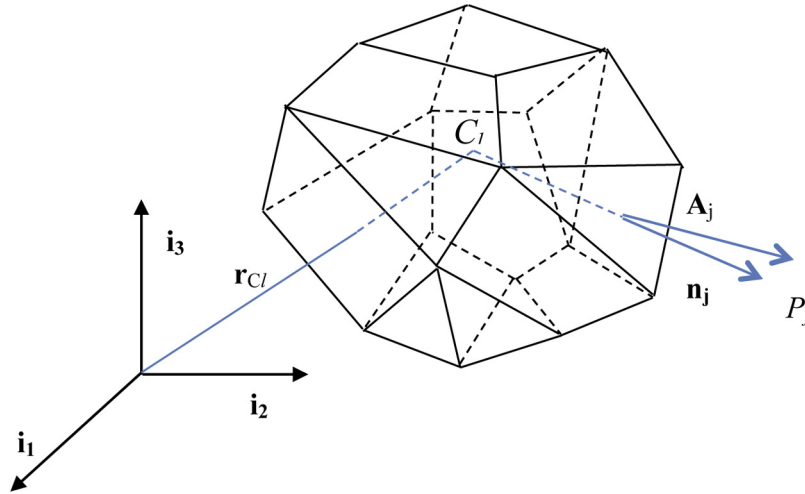


Fig. 1 – 3D view of the given finite volume.

(and equal to 6 for a cube); however during the Delaunay network discretization it can vary throughout the computational grid.

The basic idea behind the Finite Volume Method is an application of the Ostrogradski–Gauss divergence theorem to replace the volumetric integrals inherent to the governing Eq. (1) with the surface integrals rewritten for all the finite volumes completely composing the entire computational domain. A contribution of each finite volume to the global equilibrium equation is represented here as the contribution of its center as well as their outer faces, which differs from the FEM discretization, where a contribution of each element is traditionally composed from their nodal points contributions. Then, Eq. (1) is discretized in each finite volume l as

$$\left(\frac{\rho^{(\alpha)} \Delta U^{(\alpha)}}{\Delta t}\right)_l + \frac{1}{V_l} \sum_{j=1}^{n_s} \rho_j^{(\alpha)} U_j^{(\alpha)} U_j^{(\alpha)} A_j - \frac{1}{V_l} \sum_{j=1}^{n_s} \mu_j^{(\alpha)} \nabla U_j^{(\alpha)} A_j = (\nabla U^{(\alpha)})_l \nabla \mu_l^{(\alpha)} - (\nabla P^{(\alpha)})_l + \rho_l^{(\alpha)} g^{(\alpha)} \quad (24)$$

where V_l denotes obviously the l th finite volume. An exemplary finite volume of the general shape is given in Fig. 1.

The pressure gradient in x_i direction is calculated here using the Gauss integration scheme as

$$\nabla P_l^{(\alpha)}(x_i) = \frac{1}{V_l} \sum_{j=1}^{n_s} P_j^{(\alpha)} A_j n_j \quad (25)$$

where A_j is the area of the face j , n_j denotes the versor of this surface directed outwards and $\alpha = 1, \dots, M$ (as for all next equations indexed with α). We obtain analogously for the velocities

$$\nabla U_l^{(\alpha)} = \frac{1}{V_l} \sum_{j=1}^{n_s} U_j^{(\alpha)} A_j n_j \quad (26)$$

where central differencing scheme is applied to determine the given value at the cell face center. The area vectors remain constant during the response polynomials recovery as far as

the domain geometry is defined deterministically. Adopting the following definitions one may show

$$\begin{cases} K_l^{U^{(\alpha)}} = \frac{\rho_l^{(\alpha)}}{\Delta t} + \frac{1}{V_l} \sum_{j=1}^{n_s} \left\{ (1 - \chi) \rho_j^{(\alpha)} U_j^{(\alpha)} A_j + \mu_j^{(\alpha)} \frac{A_j}{|d_j|} \right\} \\ \bar{K}_{lj}^{U^{(\alpha)}} = \frac{1}{V_l} \left(\chi \rho_j^{(\alpha)} U_j^{(\alpha)} A_j - \mu_j^{(\alpha)} \frac{A_j}{|d_j|} \right) \\ Q_l^{U^{(\alpha)}} = \frac{\rho_l^{(\alpha)} U_l^{(\alpha)}(t - \Delta t)}{\Delta t} - \frac{1}{V_l} \sum_{j=1}^{n_s} P_j^{(\alpha)} A_j n_j - \rho_l^{(\alpha)} g^{(\alpha)} \\ \quad + (\nabla U_l^{(\alpha)}(t - \Delta t)) (\nabla \mu_l^{(\alpha)}(t - \Delta t)) \end{cases} \quad (27)$$

We obtain finally the algebraic equations system for the l th finite volume

$$K_l^{U^{(\alpha)}} U_l^{(\alpha)}(t) + \sum_{j=1}^{n_s} \bar{K}_{lj}^{U^{(\alpha)}} \bar{U}_{lj}^{(\alpha)}(t) = Q_l^{U^{(\alpha)}}. \quad (28)$$

The variable $\bar{U}_{lj}^{(\alpha)}(t)$ is the so-called velocity face flux adjacent to the finite volume l and its j outer plane computed at time t for the response function test indexed with α . Introduction of the face fluxes – for pressures $\bar{P}_{lj}^{(\alpha)}(t)$, temperatures $\bar{T}_{lj}^{(\alpha)}(t)$ and corresponding system matrices (marked all herein systematically with the upper bars) is specific aspect typical for the Finite Volume Method and reflects the needs of the divergence theorem. So that the global momentum equation in the RFM-based SFVM yields

$$\sum_{l=1}^N K_l^{U^{(\alpha)}} U_l^{(\alpha)}(t) + \sum_{l=1}^N \sum_{j=1}^{n_s} \bar{K}_{lj}^{U^{(\alpha)}} \bar{U}_{lj}^{(\alpha)}(t) = \sum_{l=1}^N Q_l^{U^{(\alpha)}}. \quad (29)$$

The central differencing scheme with the coefficient χ as the (linear) interpolation factor connecting the given finite volume and its particular face j is introduced here to evaluate the given scalar field at the cell face center. There holds

$$U_{jl} = U_j \chi + U_l (1 - \chi) \quad (30)$$

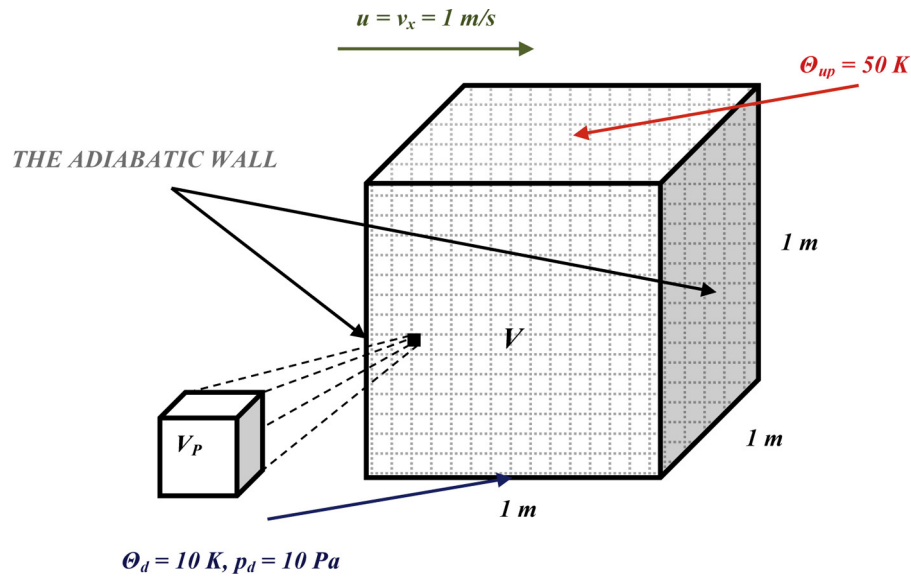


Fig. 2 – Boundary conditions for the test cube.

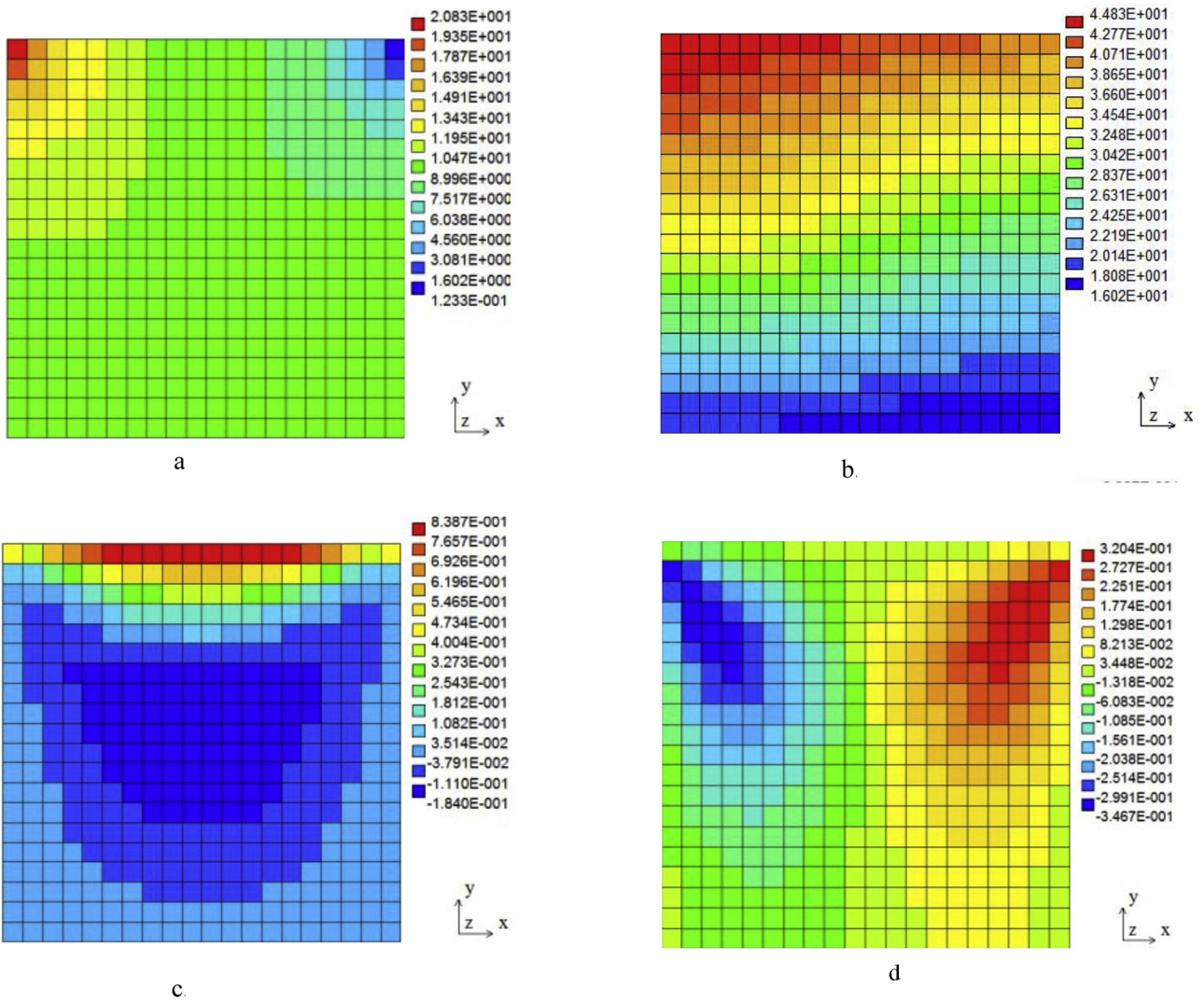


Fig. 3 – (a) Expected value of the pressures $E[p]$ for random viscosity. (b) Expected value of the temperatures $E[\theta]$ for random viscosity. (c) Expected value of horizontal velocities $E[u]$ for random viscosity. (d) Expected value of vertical velocities $E[v]$ for random viscosity.

We discretize similarly the continuity Eq. (2) on the finite volume level as

$$\sum_{j=1}^{n_s} U_j^{(\alpha)} A_j = 0. \tag{31}$$

Analogous considerations as before lead us to the following matrix equation for pressures (rewritten for the finite volumes centers contribution and the finite volumes faces separately) at the discrete level:

$$K_l^{P(\alpha)} P_l^{(\alpha)}(t) + \sum_{j=1}^{n_s} \bar{K}_{lj}^{P(\alpha)} \bar{P}_{lj}^{(\alpha)}(t) = Q_l^{P(\alpha)} \tag{32}$$

having the global form

$$\sum_{l=1}^N K_l^{P(\alpha)} P_l^{(\alpha)}(t) + \sum_{l=1}^N \sum_{j=1}^{n_s} \bar{K}_{lj}^{P(\alpha)} \bar{P}_{lj}^{(\alpha)}(t) = \sum_{l=1}^N Q_l^{P(\alpha)}. \tag{33}$$

Finally, the SFVM discretization of the heat transfer Eq. (4) is provided as

$$K_l^{T(\alpha)} T_l^{(\alpha)}(t) + \sum_{j=1}^{n_s} \bar{K}_{lj}^{T(\alpha)} \bar{T}_{lj}^{(\alpha)}(t) = Q_l^{T(\alpha)}, \tag{34}$$

where it is assumed that

$$\begin{cases} K_l^{T(\alpha)} = \frac{\rho_l^{(\alpha)} c_l^{(\alpha)}}{\Delta t} + U_{li}^{(\alpha)} \frac{1}{V_l} \rho_l^{(\alpha)} c_l^{(\alpha)} \sum_{j=1}^{n_s} \left\{ (1 - \chi) A_{lj} n_{lji} + k_l^{(\alpha)} \frac{A_j}{|d_j|} \right\} \\ \bar{K}_{lj}^{T(\alpha)} = U_{li}^{(\alpha)} \frac{1}{V_l} \rho_l^{(\alpha)} c_l^{(\alpha)} \chi A_{lj} n_{lji}, \quad i = 1, 2, 3 \\ Q_l^{T(\alpha)} = \frac{\rho_l^{(\alpha)} c_l^{(\alpha)}}{\Delta t} T_l^{(\alpha)}(t - \Delta t) + \phi_l^{(\alpha)} \end{cases} \tag{35}$$

and $\phi_l^{(\alpha)}$ is the viscous dissipation in the l th finite volume and in the α th RFM numerical test. The global heat transfer equation for the SFVM yields

$$\sum_{l=1}^N K_l^{T(\alpha)} T_l^{(\alpha)}(t) + \sum_{l=1}^N \sum_{j=1}^{n_s} \bar{K}_{lj}^{T(\alpha)} \bar{T}_{lj}^{(\alpha)}(t) = \sum_{l=1}^N Q_l^{T(\alpha)}. \tag{36}$$

Simultaneous solution to the system of Eqs. ((29), (34), (36)) enables for the polynomial approximation of the pressures,

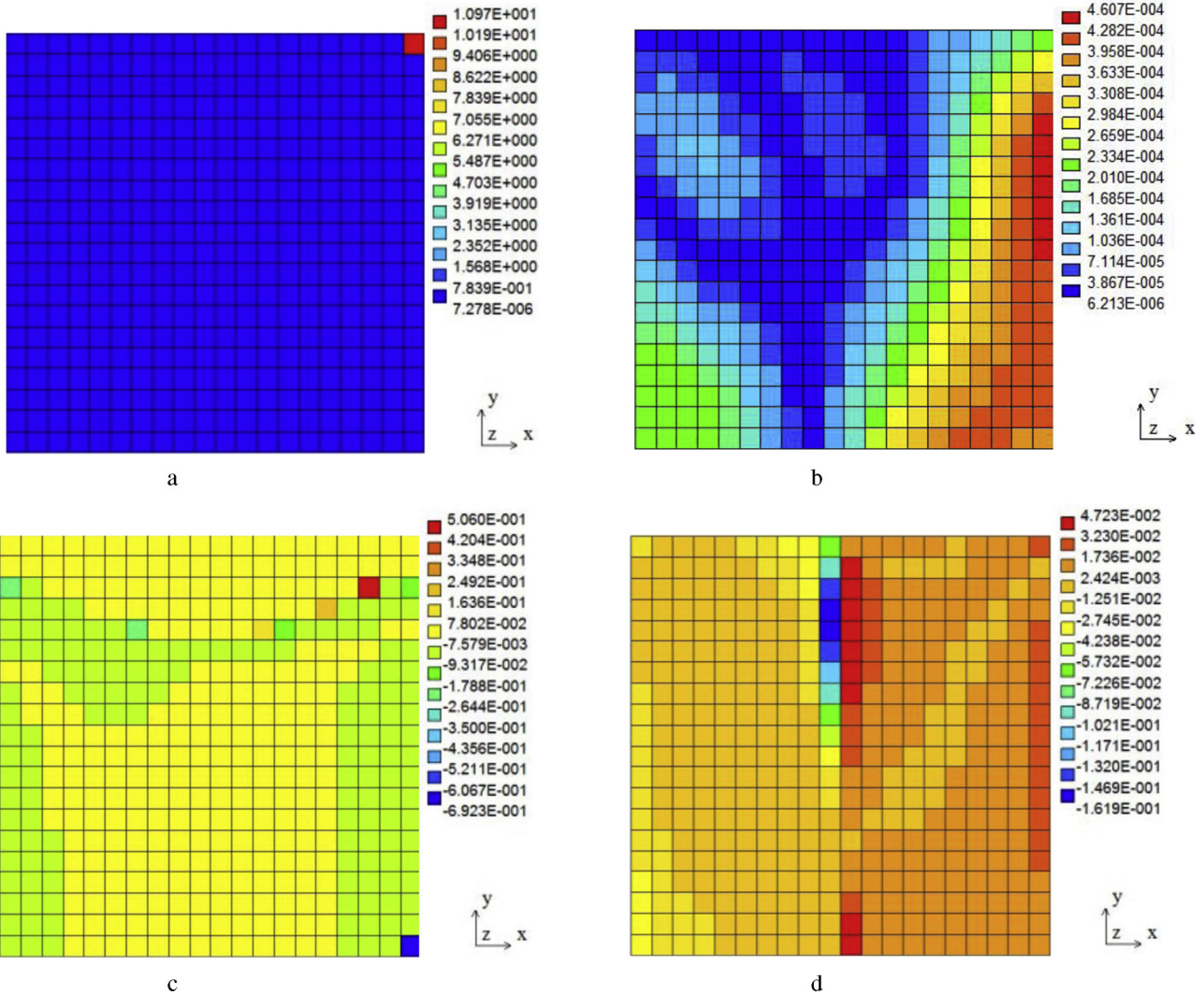


Fig. 4 – (a) Coefficient of variation of the pressures $\alpha(p)$ for random viscosity. (b) Coefficient of variation of the temperatures $\alpha(\theta)$ for random viscosity. (c) Coefficient of variation of horizontal velocities $\alpha(u)$ for random viscosity. (d) Coefficient of variation of vertical velocities $\alpha(v)$ for random viscosity.

temperatures and velocities in a fluid and final algebraic derivation of their probabilistic characteristics provided numerically in the next section. As it was mentioned, further processing of the solution toward statistical moments is performed with the use of the well-known Least Squares Method in its weighted version, which has been displayed in [2,5], for instance.

4. Computational analysis

4.1. Random viscosity modeling

Let us consider a cube of unit dimensions divided into 400 equal cubic finite volumes containing a fluid with the following physical parameters – density $\rho = 1 \text{ kg/m}^3$, specific heat $c = 100 \text{ J/kg}\cdot\text{K}$, coefficient of thermal conductivity expectation $E[k] = 10 \text{ W/m}\cdot\text{K}$ and the expected value of viscosity $E[\mu] = 10^{-1} \text{ Pa}\cdot\text{s}$ (their coefficients of variation equal both 0.15).

These two parameters are randomized separately according to the Gaussian distribution to distinguish an influence of their uncertainty on (P, V, T) solution of the given Navier–Stokes problem. The imposed boundary conditions for this cube are shown schematically in Fig. 2 – the problem is restricted to 2D analysis to make more apparent final visualization of the resulting state functions and their probabilistic characteristics. The time increment has been chosen as $\Delta t = 0.10 \text{ s}$ and the computations have been stopped at $t_k = 10 \text{ s}$. Similar numerical analysis has been carried out in [6] with traditional polynomial approximation methods instead of the WLSM technique. Computational analysis has been performed in three different computer systems – (a) OpenFVM [10], where deterministic problems with varying random parameters have been solved consecutively, (b) symbolic environment of the mathematical package MAPLE, where the local response functions were recovered on the basis of previous models and where statistical moments are programmed and derived as well as (c) by using the internet available freeware FEPlot 3.1

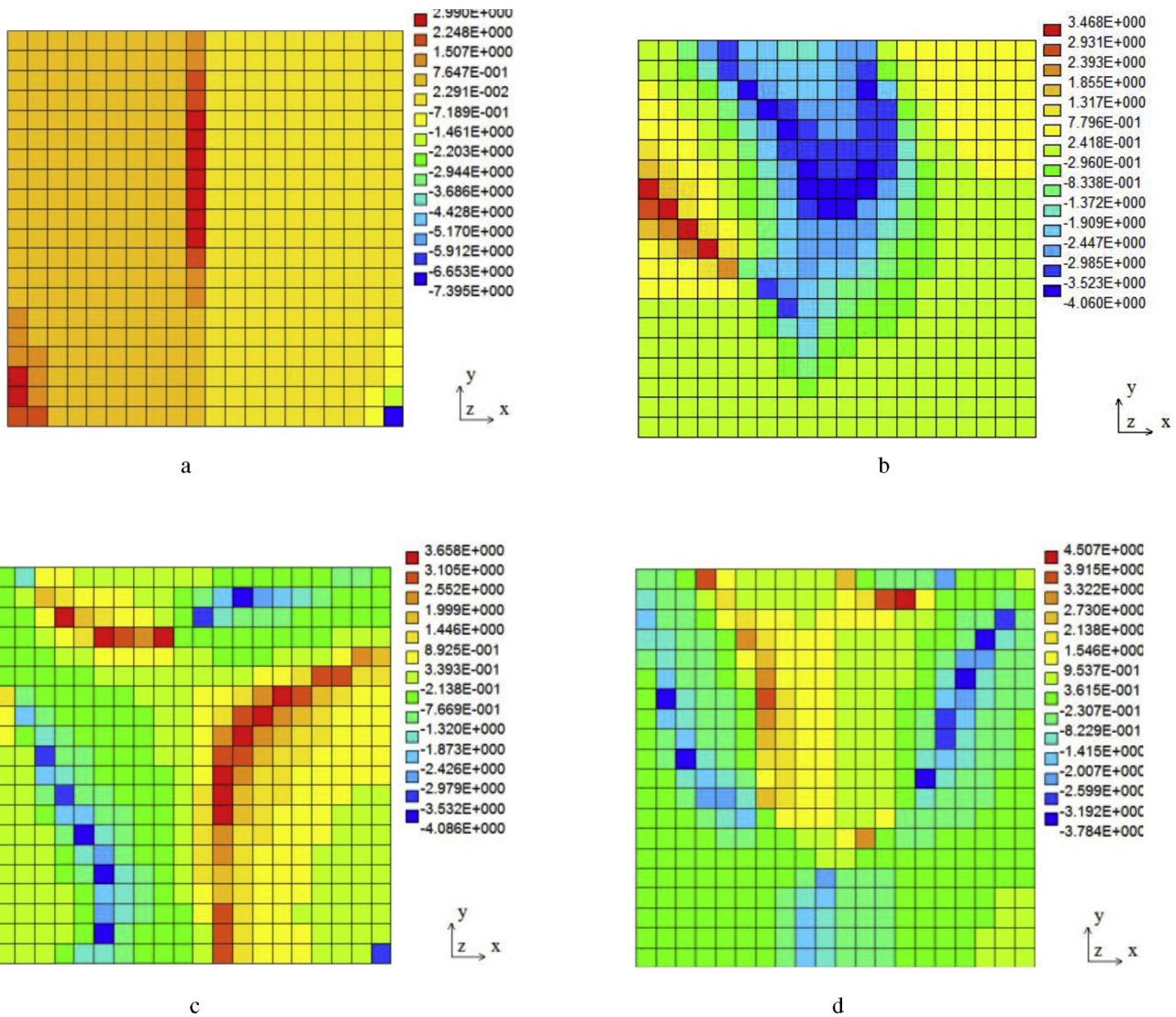


Fig. 5 – (a) Skewness coefficient of the pressures $\beta(p)$ for random viscosity. (b) Skewness coefficient of the temperatures $\beta(\theta)$ for random viscosity. (c) Skewness coefficient of horizontal velocities $\beta(u)$ for random viscosity. (d) Skewness coefficient of vertical velocities $\beta(v)$ for random viscosity.

[9], where spatial distribution of the resulting probabilistic characteristics was provided. The response functions were obtained through 11-point FVM trials in OpenFVM, where random viscosity was uniformly modified in the interval $\mu = [5 \times 10^{-2}, 15 \times 10^{-2}]$ Pa.s. Spatial distributions of the expected values, coefficients of variation, skewness and kurtosis for the pressure p , velocities in this flow (u, v) and, finally, temperature T in this domain are shown in Figs. 3-6 (from a to d, correspondingly to the state variable). Due to the fact, that this problem is really steady-state analysis its basic deterministic solution time is small and for a standard professional notebook with i7 processor is about 90 s. It makes probabilistic analysis 11 times longer plus additional time to transfer and process all the data in the system MAPLE and finally preprocess them for the FEPlot needs. The non-stationary analysis of N-S equations in deterministic version costs more than 2 h on the same processor, so that the Monte-Carlo analysis (with about 10^5 random trials) in this case would demand the very expensive parallel computing process.

The expected values given in Fig. 3 have spatial distributions and the particular values almost the same as their

deterministic counterparts reaching extremum values at the upper edge of the examined domain. As it was expected, the viscosity coefficient μ variations caused a significant change in the distribution of velocity u inside the cube test and also in pressure distribution, whereas the effect on temperature seems to be negligibly small. The largest coefficients of variation (coefficient of variation, see Fig. 4) are noticed for the horizontal velocity components, than – for the vertical one, whereas random dispersion of the pressure and temperature generally has secondary importance here. Location of the absolute maximum of these coefficients almost perfectly coincides with the minimum values of the corresponding expectations and they are usually larger than the input coefficient of variation for the fluid viscosity. The most regular spatial distribution of this probabilistic parameter is detected for the temperature field, however the values are practically negligible here, which is expected since the randomness propagates into it according to the coupling with the fluid transport equation only.

Higher order statistics (cf. Figs. 5 and 6) form quite irregular patterns in the domain analyzed, where dominating part of the PVT solution remains Gaussian (according to the skewness

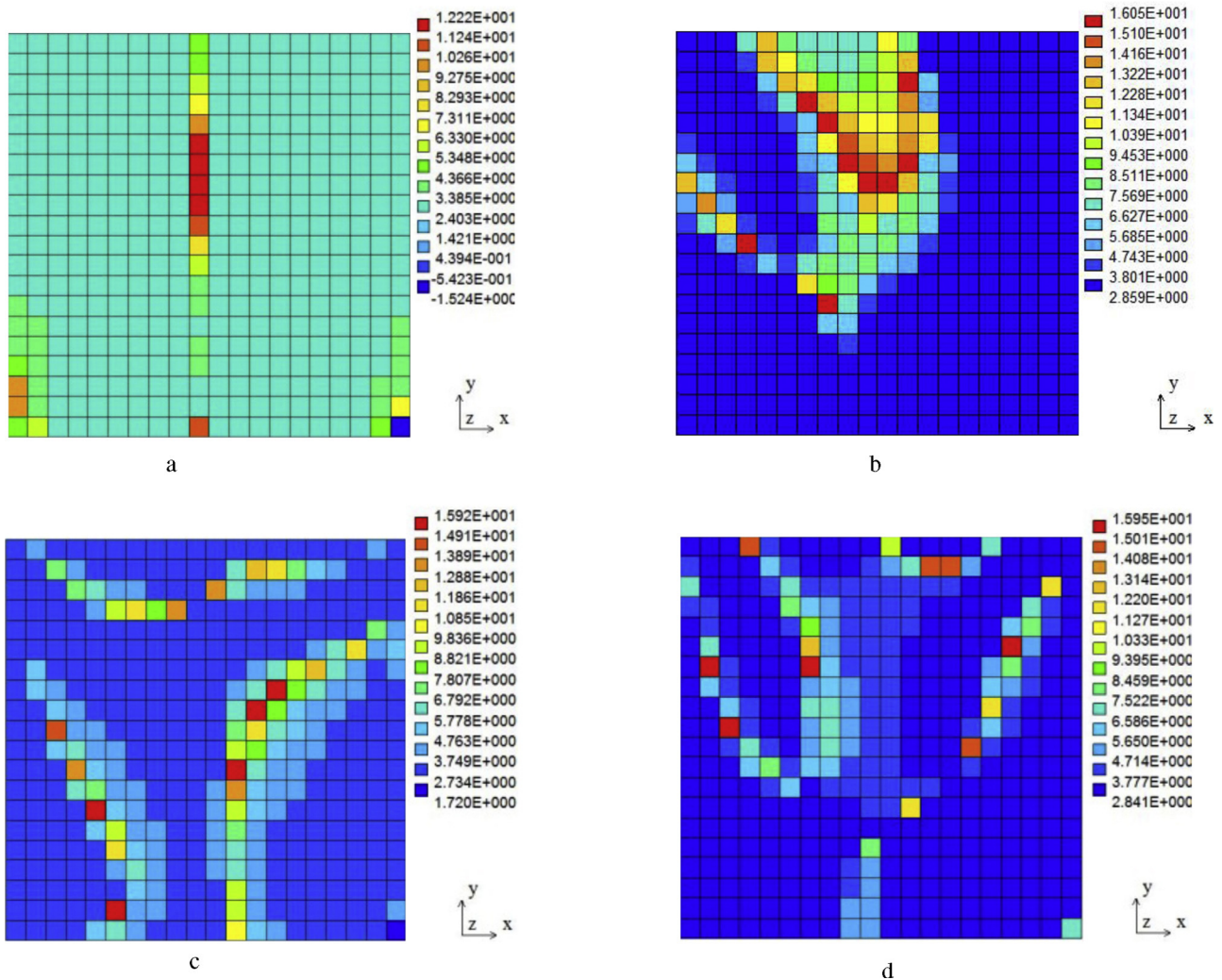


Fig. 6 – (a) Kurtosis of the pressures $\kappa(p)$ for random viscosity. (b) Kurtosis of the temperatures $\kappa(\theta)$ for random viscosity. (c) Kurtosis of horizontal velocities $\kappa(u)$ for random viscosity. (d) Kurtosis of vertical velocities $\kappa(v)$ for random viscosity.

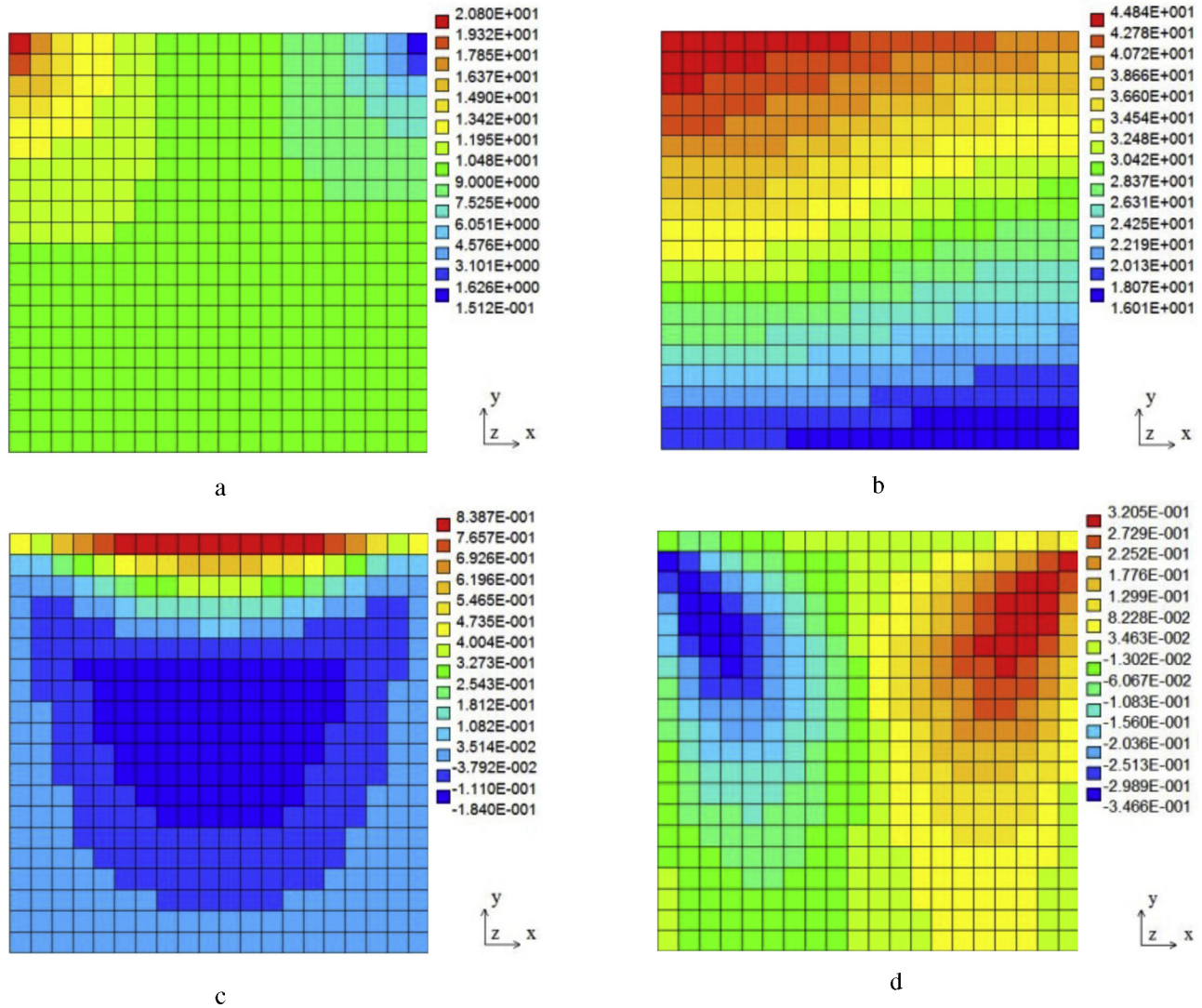


Fig. 7 – (a) Expected value $E[p]$ for random heat conductivity. (b) Expected value $E[\theta]$ for random heat conductivity. (c) Expected value $E[u]$ for random heat conductivity. (d) Expected value $E[v]$ for random heat conductivity.

and kurtosis). However, maximum values of both coefficients may be even many times more than the values adequate to the normal probability density function and appear in the exceptional cases only. A detailed comparison of Figs. 5a and 6a and the remaining pairs of these probabilistic characteristics shows clearly that the patterns of skewness and kurtosis for the specific components of the PVT solution almost strictly coincide, so that the larger deviations from the values typical Gaussian distribution in both cases have the same location in this domain.

4.2. Random heat conductivity coefficient

Quite a similar analysis was conducted using constant viscosity value $\mu = 10^{-2}$ Pa·s, given parameters ρ, c, β and the coefficient of thermal conductivity taken as the input Gaussian random variable with the same coefficient of variation and the expectation equal to $E[k] = 10$ W/m·K; analogously as in Section 4.1 we provide 11 deterministic solutions with

$k \in [5 \dots 15]$ W/m·K. The results obtained (expectations, coefficients of variation, skewness and kurtosis) for the temperature θ , flow velocity $v_x \equiv u, v_y \equiv v$ and pressure p show illustrations Figs. 7a, d and 8–10. Assumed variations of the thermal conductivity coefficient k cause a significant reduction in the temperature difference $\Delta\theta = \theta_{up} - \theta_d$ (see Fig. 2). The other physical quantities – u, v and p are totally independent from this parameter and that is why the detailed statistical analysis and visualization were conducted only for temperature θ .

As it is typical for the stochastic perturbation-based methods, the expectations of the state functions computed at the mean values of various probabilistic parameters are exactly the same – one may compare Fig. 3a against Fig. 7a, etc. Some small exceptions at the minimum values follow rather the discrepancies of the deterministic computer technique itself. Contrary to the previous cases now all higher order characteristics – variation coefficient, skewness and kurtosis all have the very regular spatial distributions without any local

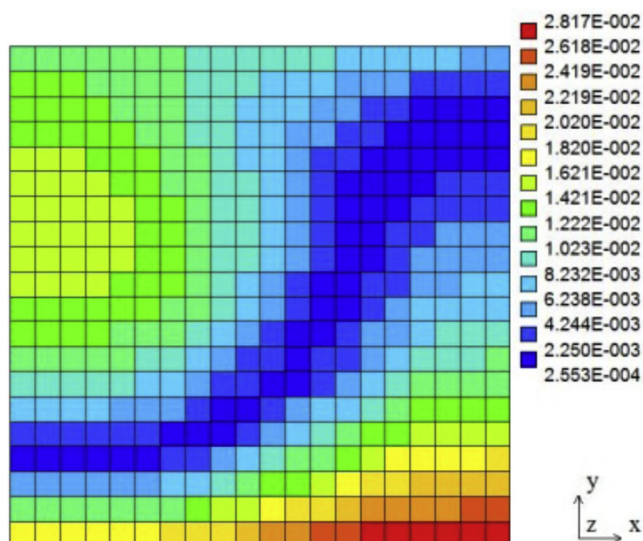


Fig. 8 – Coefficient of variation $\alpha(\theta)$ for random heat conductivity.

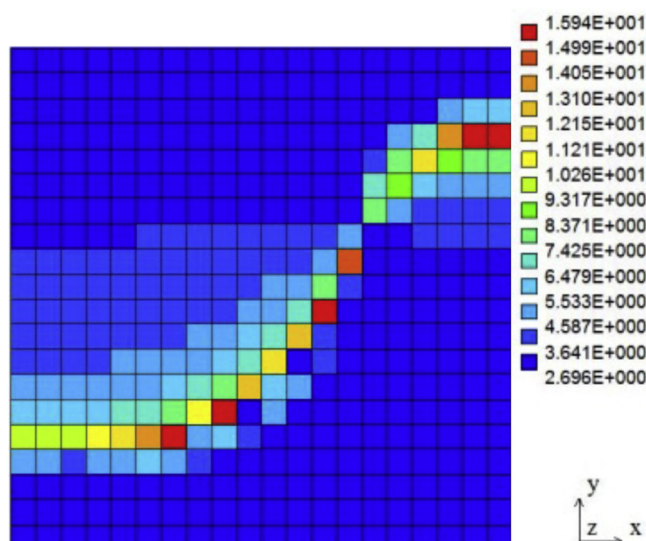


Fig. 10 – Kurtosis $\kappa(\theta)$ for random heat conductivity.

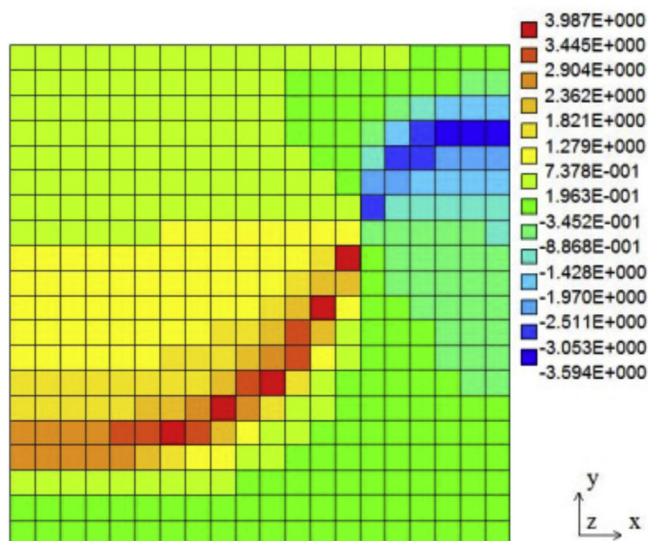


Fig. 9 – Skewness $\beta(\theta)$ for random heat conductivity.

large gradients and outstanding extremum values. Since that the extremum values within these coefficients all coincide with each other and, further, the uncertainty at the output temperature field is significantly smaller than the input coefficient of variation for the heat conductivity. Particular values of skewness and kurtosis show that the temperature has a distribution very distant from the Gaussian, so that the first two moments information is not sufficient to characterize it uniquely.

5. Concluding remarks

(1) The Stochastic perturbation-based Finite Volume Method proposed in this paper in conjunction with the discrete Response Function Method based on the Weighted Least

Squares Method seems to be an efficient alternative to both Monte-Carlo simulation technique and stochastic polynomial chaos expansions. The overall numerical error inherent in the Direct Differentiation Method version of the perturbation-based SFEM and resulting from the solution to the increasing order hierarchical equations is reduced after an application of the RFM technique. Now, the proposed technique deficiency equivalent to approximation error by only, which was additionally decreased by the weighted least squares technique itself. The values of most of probabilistic moments obtained with the use of the weighted version of the LSM were slightly smaller than these returned by the non-weighted approach presented in [6], but their patterns remained almost the same.

(2) Generally, the method presented enables for randomization of the deterministic FVM models with multi-component random vectors also with both uncorrelated and correlated components, but then the additional cross-correlations need to be given and inserted into the equations for all the statistical moments of state parameters. Randomization of the non-linear problems with state-dependent physical parameters of the fluids does not seem to be straightforward but uncertainty propagation step-by-step in such a computational analysis may make higher order statistics extremely large. It can be concluded from the numerical illustration recalled above, where some extreme values of the skewness and kurtosis maxima have been detected that are very distant from the zeroes adjacent to the Gaussian PDF.

REFERENCES

[1] H.S. Carslaw, J.C. Jaeger, *Conduction of Heat in Solids*, Oxford Sci. Pub., Clarendon Press, Oxford, 1986.
 [2] L. Cueto-Felgueroso, I. Colominas, X. Nogueira, M. Casteleiro, *Finite volume solvers and Moving Least-Squares approximations for the compressible Navier-Stokes equations*

- on unstructured grids, *Computer Methods in Applied Mechanics and Engineering* 196 (2007) 4712-4736.
- [3] I. Demirdzic, S. Muzaferija, Numerical method for coupled fluid flow, heat transfer and stress analysis using unstructured moving meshes with cells of arbitrary topology, *Computer Methods in Applied Mechanics and Engineering* 125 (1995) 235-255.
- [4] J. Durany, J. Pereira, F. Varas, A cell-vertex finite volume method for thermo-hydrodynamic problems in lubrication theory, *Computer Methods in Applied Mechanics and Engineering* 195 (2006) 5949-5961.
- [5] M. Kamiński, *The Stochastic Perturbation Method for Computational Mechanics*, Wiley, Chichester, 2013.
- [6] M. Kamiński, R.L. Ossowski, On application of the Stochastic Finite Volume Method in some Navier-Stokes problems, *Computer Modeling in Engineering and Sciences* 80 (1) (2011) 113-140.
- [7] M. Kamiński, G.F. Carey, Stochastic perturbation-based finite element approach to fluid flow problems, *International Journal of Numerical Methods for Heat & Fluid Flow* 15 (2005) 671-697.
- [8] M. Schäfer, *Computational Engineering – Introduction to Numerical Methods*, Springer-Verlag, Berlin, 2006.
- [9] [http://vbn.aau.dk/en/persons/erik-lun\(eacec6ff-lb29-4366-a9ee-35a1b28a95b5\).html](http://vbn.aau.dk/en/persons/erik-lun(eacec6ff-lb29-4366-a9ee-35a1b28a95b5).html).
- [10] <http://openfvm.sourceforge.net>.